

Pairing Correlations in Nuclei on Neutron Drip Line

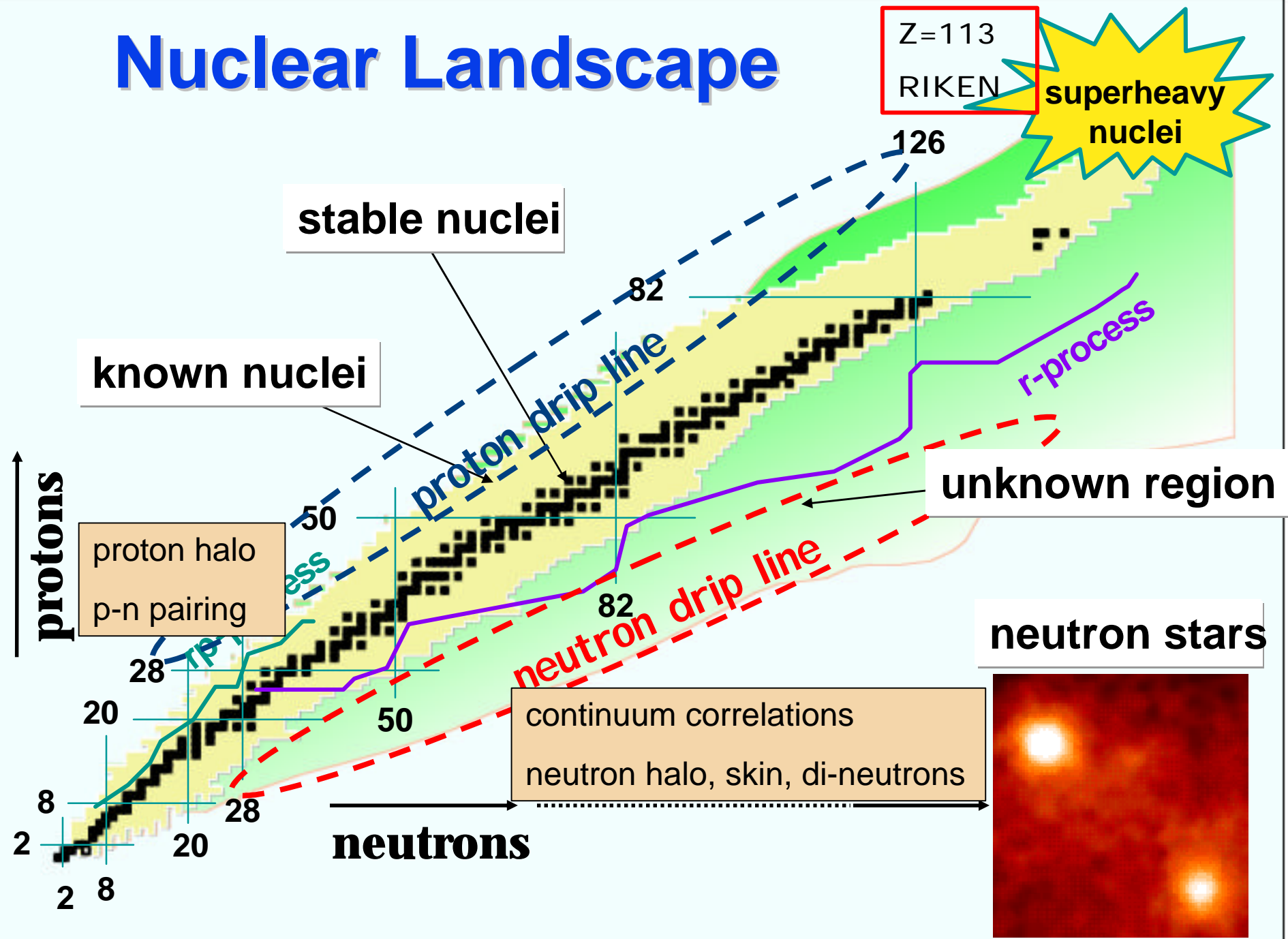
INT Workshop on Pairing degrees of freedom in nuclei and the nuclear medium
Nov. 14-17, 2005

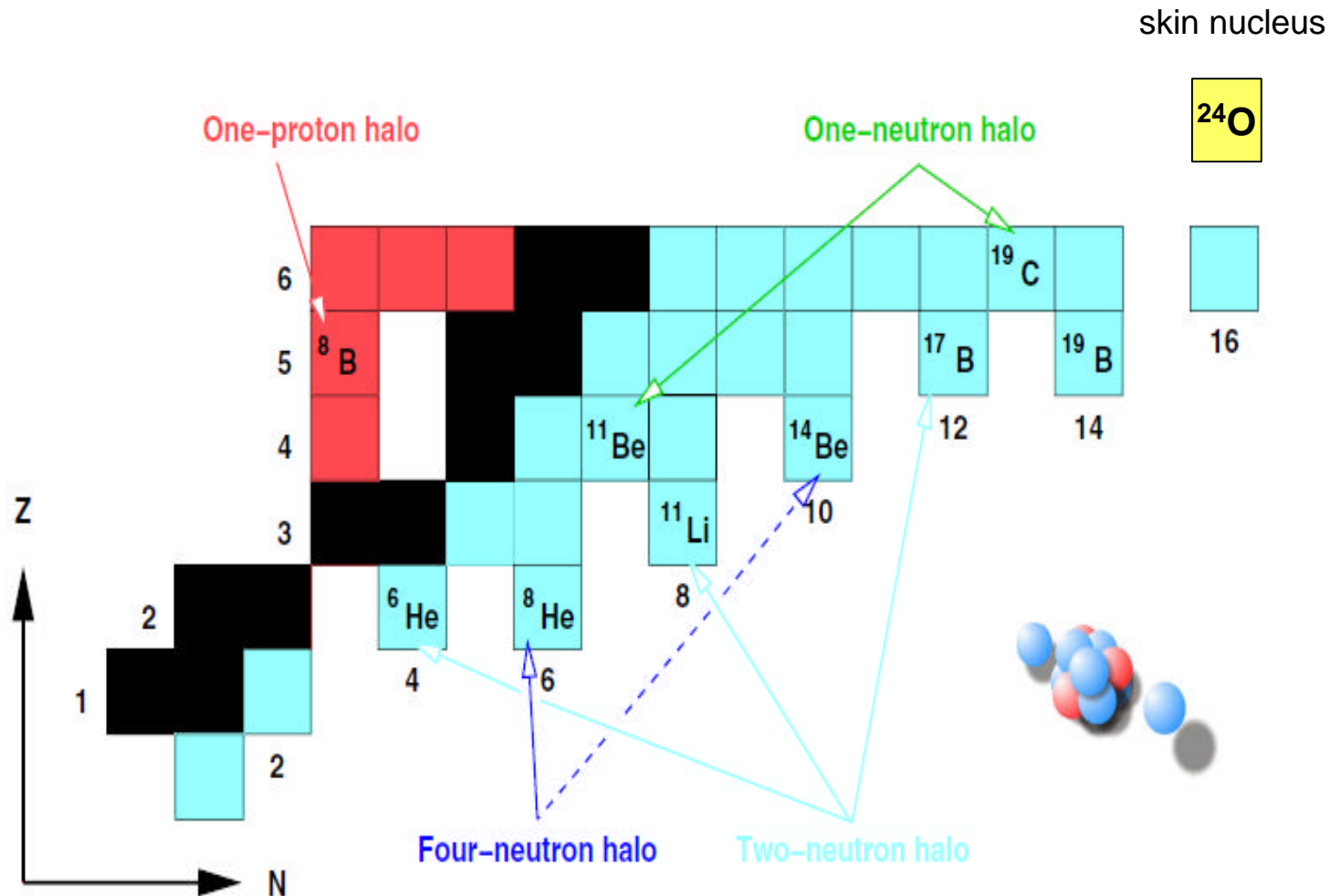
Hiroyuki Sagawa (University of Aizu)

- Introduction
- Three-body model
- Di-neutron and H₂O molecule (cigar) -type configurations
- Summary

collaborator: K. Hagino (Tohoku University)

Nuclear Landscape



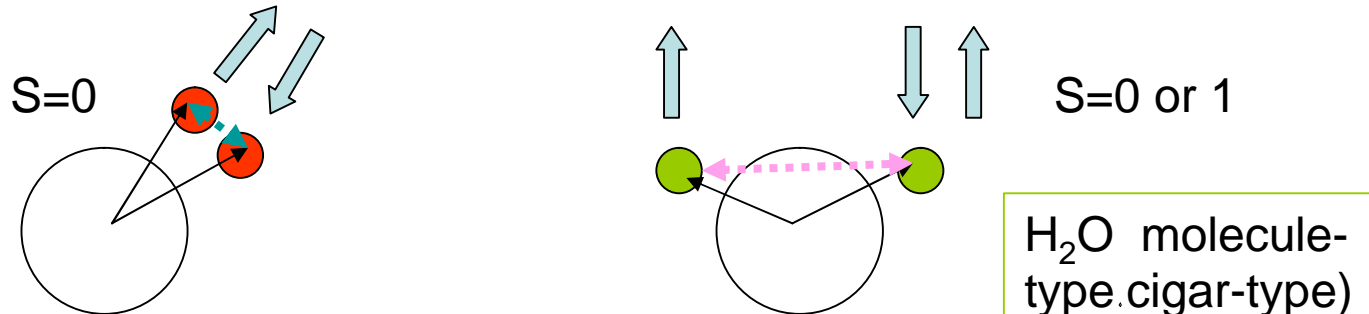


Pairing correlations in nuclei on the neutron drip line - Borromean systems -

K. Hagino and H. Sagawa

Phys. Rev. C72,044321(2005)

1. Three body model with a density-dependent delta-interaction
2. Ground states of borromean nuclei ${}^6\text{He}$ and ${}^{11}\text{Li}$ and a skin nucleus ${}^{24}\text{O}$
halo vs. skin
di-neutron vs. molecule configurations
3. Dipole excitations
4. Summary



Three-body model

(Bertsch-Esbensen, Ann.Phys.209,327(1991), Nucl.Phys.A542, 310 (1992).)

The single-particle Hamiltonian for a neutron interacting with the core is

$$h_{nc} = \frac{p^2}{2\mu} + V_{nc}(r), \quad (3.2)$$

where $\mu = m A_c / (A_c + 1)$ is the reduced mass. The three-body Hamiltonian then takes the form

$$H = h_{nc}(1) + h_{nc}(2) + V_{nn} + \frac{\mathbf{p}_1 \cdot \mathbf{p}_2}{A_c m}. \quad (3.3)$$

$$V_{nn} = \delta(\mathbf{r}_1 - \mathbf{r}_2) \left(v_0 + \frac{v_\rho}{1 + \exp[(r_1 - R_\rho)/a_\rho]} \right).$$

$$v_0 = 2\pi^2 \frac{\hbar^2}{m} \alpha = 2\pi^2 \frac{\hbar^2}{m} \frac{2a_{nn}}{\pi - 2k_c a_{nn}}.$$

where $a_{nn} = -15\text{fm}$ is nn scattering length and k_c is determined by the effective range, while v_r , R_r and a_r are adjusted in order to reproduce known ground state properties of each nucleus.

Parameters of V_{n-C} and V_{n-n} interactions

$$V_{nC}(r) = V_0 \left[1 - 0.44 f_{so} r_o^2 (\vec{l} \cdot \vec{s}) \right] \frac{1}{r} \frac{d}{dr} \left(\frac{1}{1 + \exp((r - R)/a)} \right)$$

with $R = r_o A_C^{1/3}$ fm.

V_{nc}	V _o (MeV)	r _o (fm)	a (fm)	f _{so}
⁶ He	-47.4	1.25	0.65	0.93
¹¹ Li (-parity) (+parity)	-35.366	1.27	0.67	1.006
	-47.5			
²⁴ O	-43.2	1.25	0.67	0.73

V_{nn}	ν_o (MeVfm ³)	ν_r (MeVfm ³)	R_r (fm)	a_r (fm)	E _{cut} (MeV)
⁶ He	-751.3	751.3	2.436	0.67	40
¹¹ Li	-854.2	854.2	2.935	0.67	30
²⁴ O	-854.2	814.2	3.502	0.67	30

Two neutron state for ground state

$$\Psi_{nn',\ell j}^{(2)}(\mathbf{r}_1, \mathbf{r}_2) = \sum_m \langle jmj - m | 00 \rangle \psi_{n\ell jm}(\mathbf{r}_1) \psi_{n'\ell j-m}(\mathbf{r}_2).$$

$$\tilde{\Psi}_{nn',\ell j}(\mathbf{r}_1, \mathbf{r}_2) = \frac{1}{\sqrt{2(1 + \delta_{nn'})}} [\Psi_{nn',\ell j}^{(2)}(\mathbf{r}_1, \mathbf{r}_2) + \Psi_{nn',\ell j}^{(2)}(\mathbf{r}_2, \mathbf{r}_1)]$$

where $\psi_{n\ell jm}(\mathbf{r}_1)$ is the eigenstates of single-particle Hamiltonian h_{nC} .

Neutron separation

$$\langle r_{n,n}^2 \rangle = \langle \Psi_{g.s.} | |\mathbf{r}_1 - \mathbf{r}_2|^2 | \Psi_{g.s.} \rangle$$

Di-neutron-core distance

$$\langle r_{c,2n}^2 \rangle = \langle \Psi_{g.s.} | |(\mathbf{r}_1 + \mathbf{r}_2)/2|^2 | \Psi_{g.s.} \rangle$$

Ground State Properties

nucleus	S_{2n} (MeV)	$\langle r_{nn}^2 \rangle^{1/2}$ (fm)	$\langle r_{c-2n}^2 \rangle^{1/2}$ (fm)	configuration	(%)
${}^6\text{He}$	0.975	21.3	13.2	$(p_{3/2})^2$	83.0
${}^{11}\text{Li}$	0.295	41.4	26.3	$(p_{1/2})^2$	59.1
				$(s_{1/2})^2$	22.7
${}^{24}\text{O}$	6.452	35.2	10.97	$(s_{1/2})^2$	93.6
$(e_{s1/2} = -2.739\text{MeV}, e_{d5/2} = -3.806\text{MeV})$					
${}^{11}\text{Li}$	0.376	37.7	23.7	$(p_{1/2})^2$	59.8
				$(s_{1/2})^2$	22.1

S_{2n} is still controversial in ${}^{11}\text{Li}$.

C. Bachelet et al., $S_{2n}=376\pm 5\text{keV}$ (ENAM,2004)

TABLE II. Results for ground state of ${}^6\text{He}$. The first three lines have been extracted from Ref. [12]. Our results (lines 4 and 5) were obtained for a nn scattering length of -15 fm and radial box of 30 fm as described in Sec. IV B. Lines 6 and 7 show the corresponding no-recoil limit.

Line	Comments	S_{2n} (keV)	$\langle r_{c,2n}^2 \rangle$ (fm 2)	$\langle r_{n,n}^2 \rangle$ (fm 2)	$(p_{3/2})^2$ (%)	$S=0$ (%)
1	HH-GPT-WS*	985	11.7	20.3		
2	CSF-SSC-WS*	950	13.0	21.7		88.2
3	CRC-v14-KP*	974	12.3	20.7		
4	$E_{\text{cut}}=15 \text{ MeV}$	975	12.9	29.3	89.2	85.6
5	$E_{\text{cut}}=40 \text{ MeV}$	975	13.2	21.3	83.0	87.0
6	No recoil, $E_{\text{cut}}=15 \text{ MeV}$	975	10.3	29.5	92.0	86.1
7	No recoil, $E_{\text{cut}}=40 \text{ MeV}$	975	10.7	24.3	87.9	87.9

TABLE IV. Ground state properties of ${}^{11}\text{Li}$ for a binding energy of 295 keV . The radial box size was 40 fm and the adopted nn scattering length was -15 fm . Lines 1 and 2 were based on a neutron-core interaction that produces a $p_{1/2}$ resonance at 540 keV , and an s -wave scattering length of $a_{nc}=+1.7 \text{ fm}$. Line 5 was based on a stronger interaction in even-parity states, producing an s -wave scattering length of $a_{nc}=-5.6 \text{ fm}$. A particular set of Faddeev results [4], based on a $p_{1/2}$ resonance at 200 keV and a realistic nn interaction, is shown in line 3 for comparison. Line 4 is the results we obtained previously [1] in the no-recoil limit, with a two-neutron binding energy of 200 keV and a neutron-core $p_{1/2}$ resonance at 800 keV .

Line	Comments	$\langle r_{c,2n}^2 \rangle$ (fm 2)	$\langle r_{n,n}^2 \rangle$ (fm 2)	$(s_{1/2})^2$ (%)	$(p_{1/2})^2$ (%)
1	$a_{nc}=1.7 \text{ fm}$, $E_{\text{cut}}=15 \text{ MeV}$	18.7	42.8	4.5	89.1
2	$a_{nc}=1.7 \text{ fm}$, $E_{\text{cut}}=30 \text{ MeV}$	18.3	37.6	4.6	85.3
3	Q9 of Ref. [4]	21.2	44.9		
4	Ref. [1], no recoil	24.3	39.0	6.1	76.9
5	$a_{nc}=-5.6 \text{ fm}$, $E_{\text{cut}}=15 \text{ MeV}$	26.2	45.9	23.1	61.0

Two-body Density

$$\begin{aligned}\mathbf{r}_2(r_1, r_2, \mathbf{q}_{12}) &= \left\langle \Psi_{gs}(\overrightarrow{r_1}, \overrightarrow{r_2}) \middle| \Psi_{gs}(\overrightarrow{r_1}, \overrightarrow{r_2}) \right\rangle \\ &= \mathbf{r}_2^{S=0}(r_1, r_2, \mathbf{q}_{12}) + \mathbf{r}_2^{S=1}(r_1, r_2, \mathbf{q}_{12})\end{aligned}$$

One-body density as a function of angle

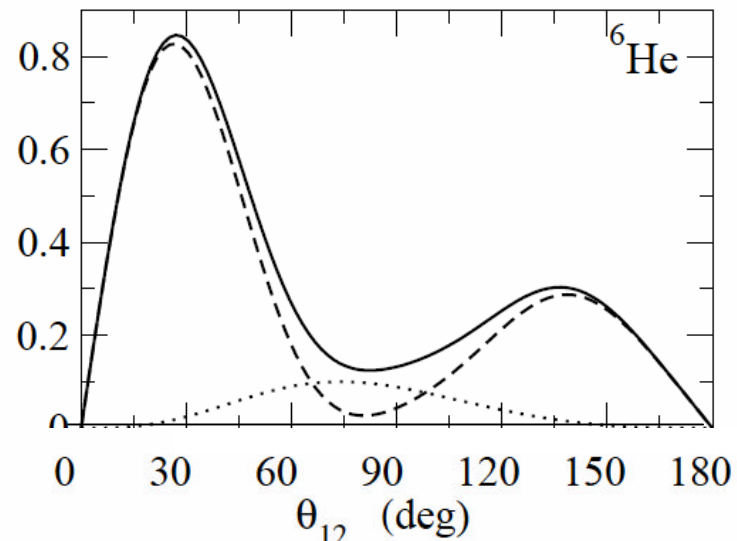
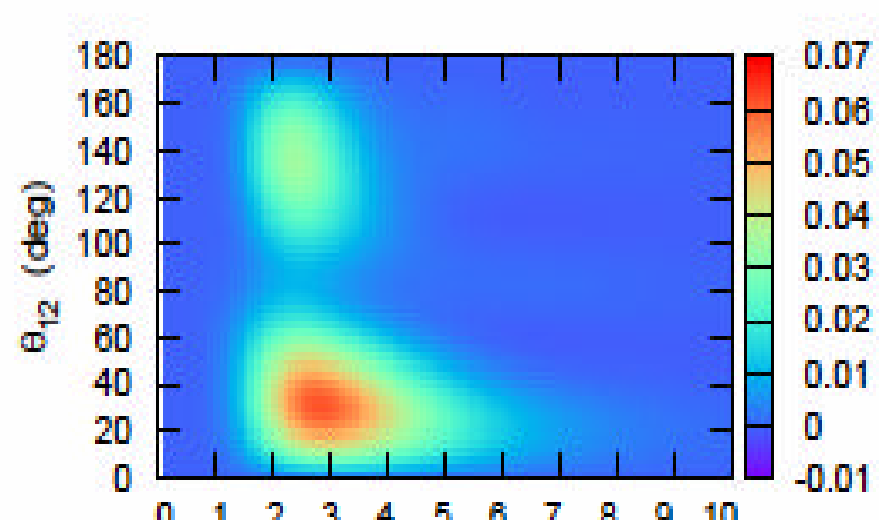
$$\mathbf{r}(\mathbf{q}_{12}) \equiv 4\mathbf{p} \int_0^{\infty} r_1^2 dr_1 \int_0^{\infty} r_2^2 dr_2 \mathbf{r}_2(r_1, r_2, \mathbf{q}_{12})$$

Spin decomposition of two-body density

$$\begin{aligned}
 \mathbf{r}_2^{S=0}(r_1, r_2, \mathbf{q}_{12}) = & \frac{1}{8\mathbf{p}} \sum_{L, l, j, l' j'} \frac{\hat{l} \hat{l}' \hat{L}}{\sqrt{4\mathbf{p}}} \begin{pmatrix} l & l' & L \\ 0 & 0 & 0 \end{pmatrix}^2 \\
 & \times (-)^{l+l'} \sqrt{\frac{2j+1}{2l+1}} \sqrt{\frac{2j'+1}{2l'+1}} \Phi_{lj}(r_1, r_2) \Phi_{l'j'}(r_1, r_2) Y_{L0}(\mathbf{q}_{12})
 \end{aligned}$$

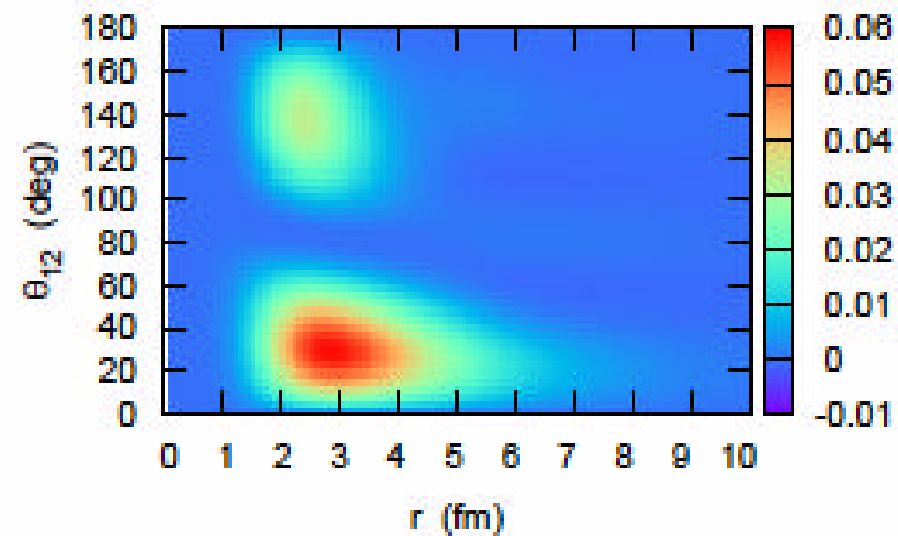
$$\begin{aligned}
 \mathbf{r}_2^{S=1}(r_1, r_2, \mathbf{q}_{12}) = & \frac{1}{8\mathbf{p}} \sum_{L, l, j, l' j'} \frac{\hat{l} \hat{l}' \hat{L}}{\sqrt{4\mathbf{p}}} \begin{pmatrix} l & l' & L \\ 0 & 0 & 0 \end{pmatrix} \begin{pmatrix} l & l' & L \\ 1 & -1 & 0 \end{pmatrix} \\
 & \times (-)^{j+j'} \sqrt{2 - \frac{2j+1}{2l+1}} \sqrt{2 - \frac{2j'+1}{2l'+1}} \Phi_{lj}(r_1, r_2) \Phi_{l'j'}(r_1, r_2) Y_{L0}(\mathbf{q}_{12})
 \end{aligned}$$

Total

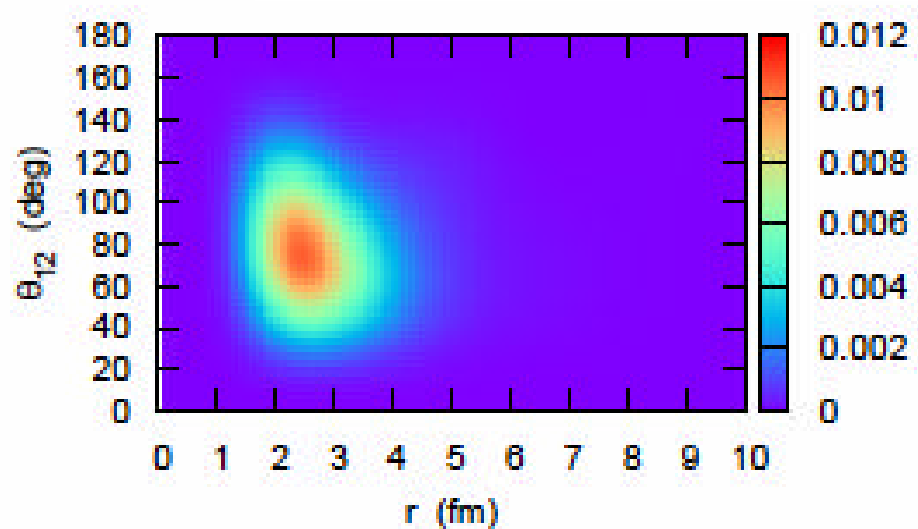


$S=0$

r (fm)



$S=1$



Two-body Density

$$\begin{aligned}\mathbf{r}_2(r_1, r_2, \mathbf{q}_{12}) &= \left\langle \Psi_{gs}(\overrightarrow{r_1}, \overrightarrow{r_2}) \middle| \Psi_{gs}(\overrightarrow{r_1}, \overrightarrow{r_2}) \right\rangle \\ &= \mathbf{r}_2^{S=0}(r_1, r_2, \mathbf{q}_{12}) + \mathbf{r}_2^{S=1}(r_1, r_2, \mathbf{q}_{12})\end{aligned}$$

One-body density as a function of angle

$$\mathbf{r}(\mathbf{q}_{12}) \equiv 4\mathbf{p} \int_0^{\infty} r_1^2 dr_1 \int_0^{\infty} r_2^2 dr_2 \mathbf{r}_2(r_1, r_2, \mathbf{q}_{12})$$

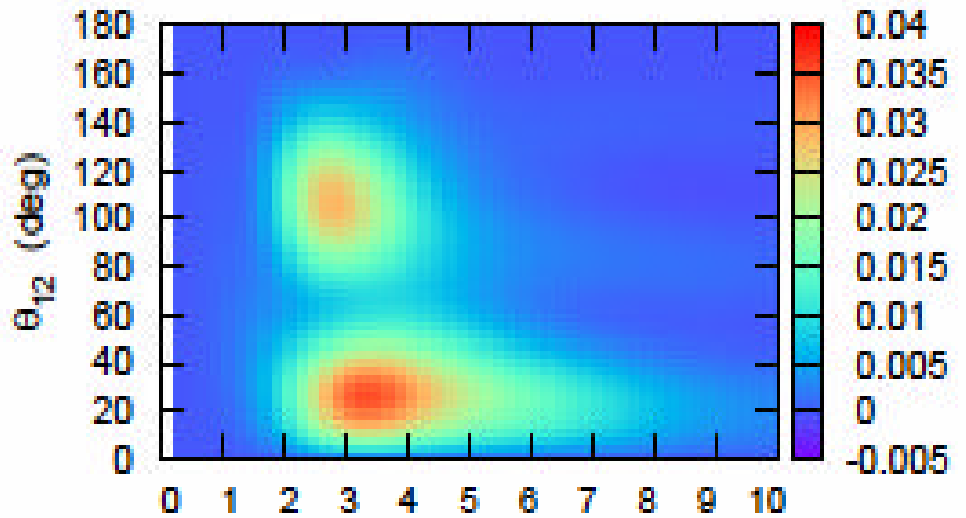
For $(p)^2$ J=0 configuration, S=0 and S=1 contributions (Talmi-Moshinsky transformation);

$$\sin(\mathbf{q}_{12}) \mathbf{r}_2^{S=0}(\mathbf{q}_{12}) \propto \sin(\mathbf{q}_{12}) \text{con}^2(\mathbf{q}_{12}) \quad \text{Peaked at } 35^\circ \text{ and } 145^\circ$$

$$\sin(\mathbf{q}_{12}) \mathbf{r}_2^{S=1}(\mathbf{q}_{12}) \propto \sin^3(\mathbf{q}_{12}) \quad 90^\circ$$

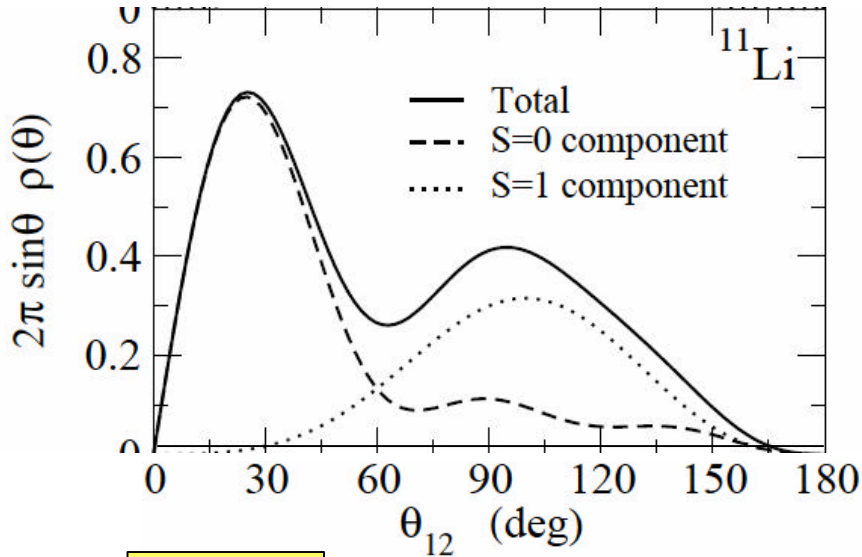
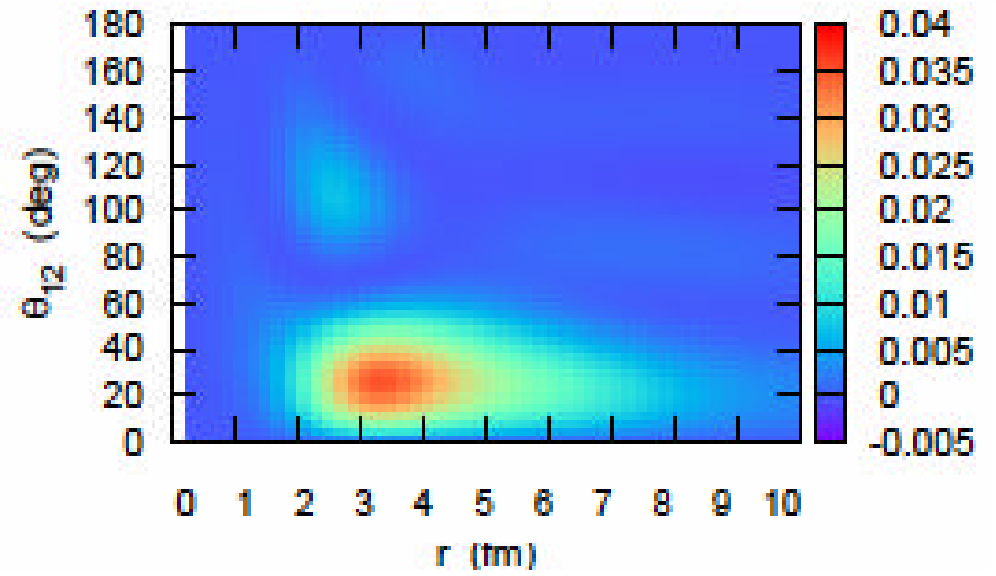
For $(s)^2$ J=0 configuration, only S=0 is possible.

Total

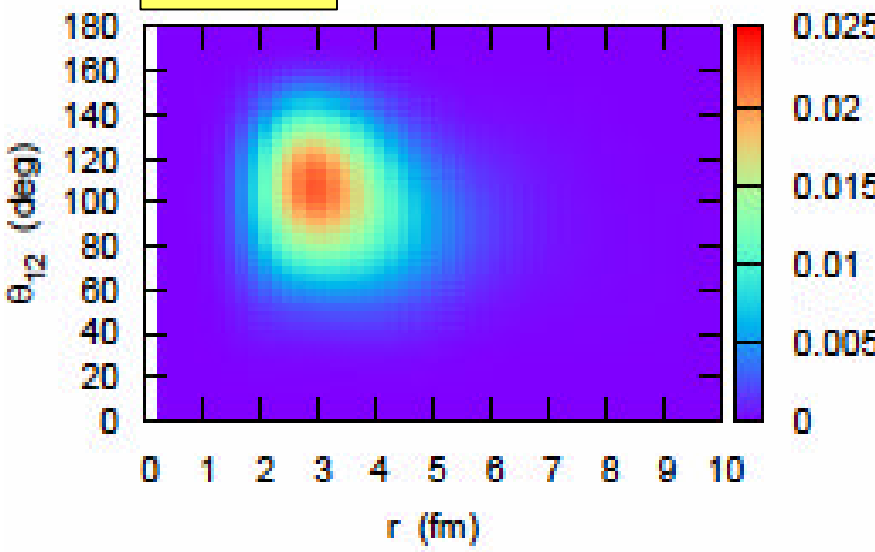


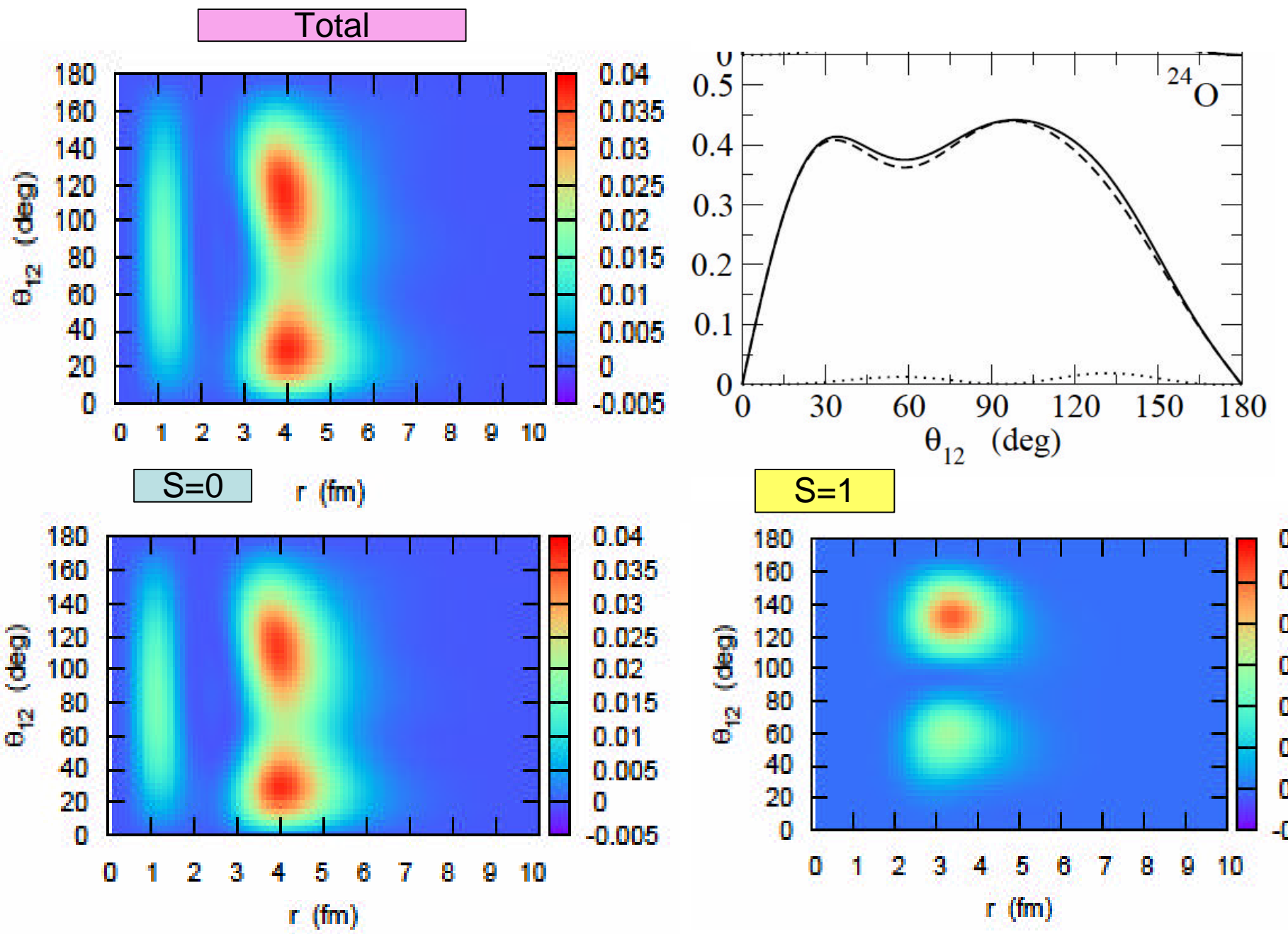
S=0

r (fm)



S=1





Average correlation angles

	^6He	^{11}Li	^{24}O
\mathbf{J}_{12}	66.3°	65.3°	82.7°

Anti-halo effect in ^{24}O

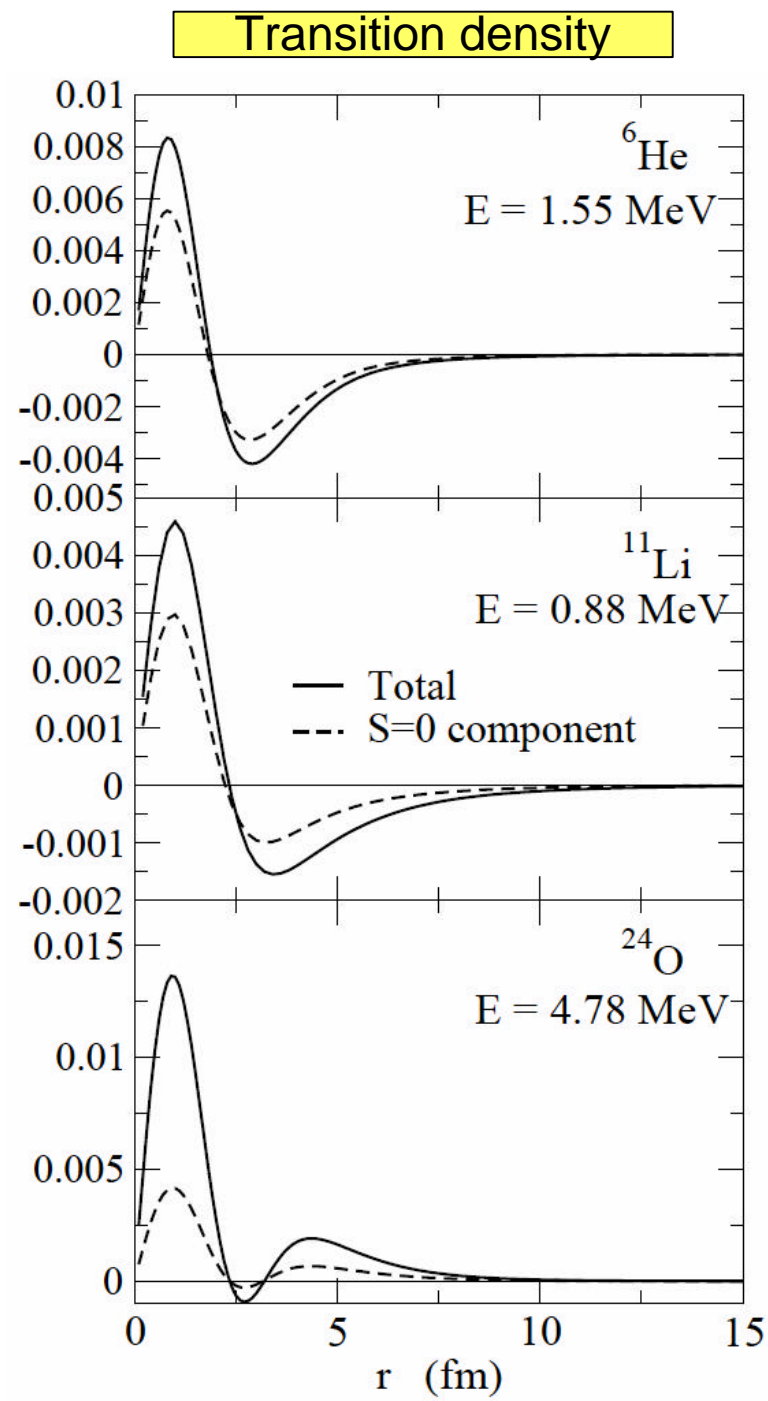
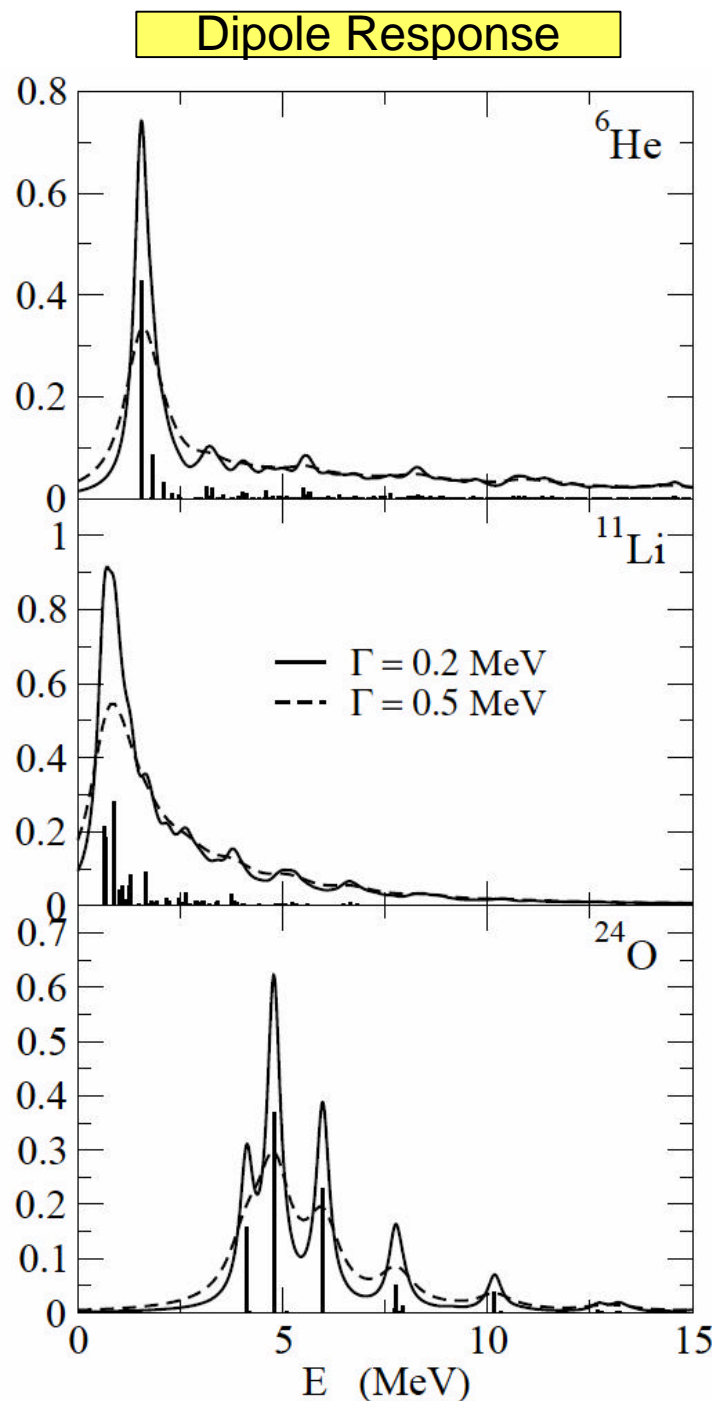
$$r_m (2n) = 4.45 \text{ fm} \quad r(2s_{1/2}) = 4.65 \text{ fm}$$

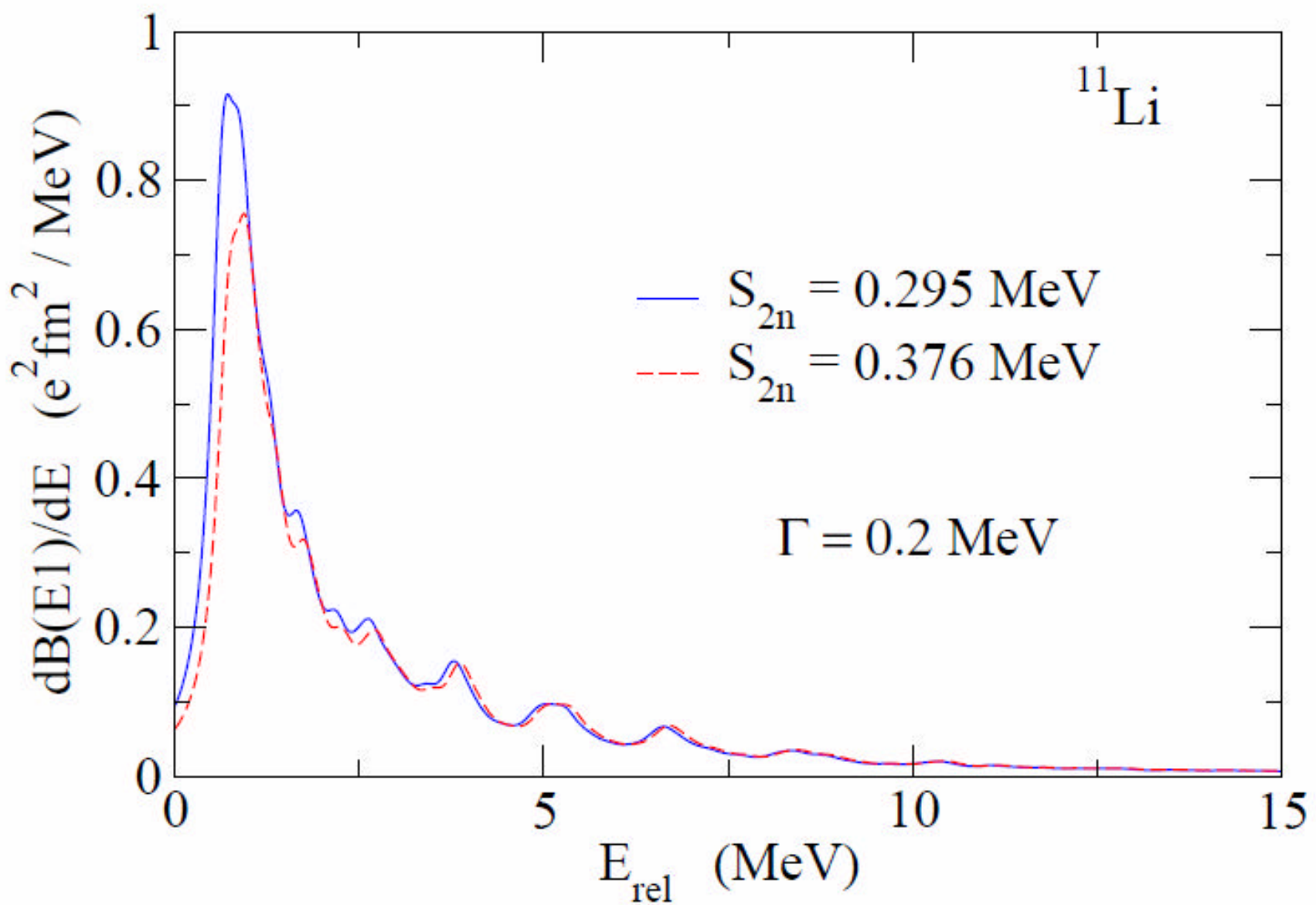
How can we observe di-neutron and H₂ O-type configurations?

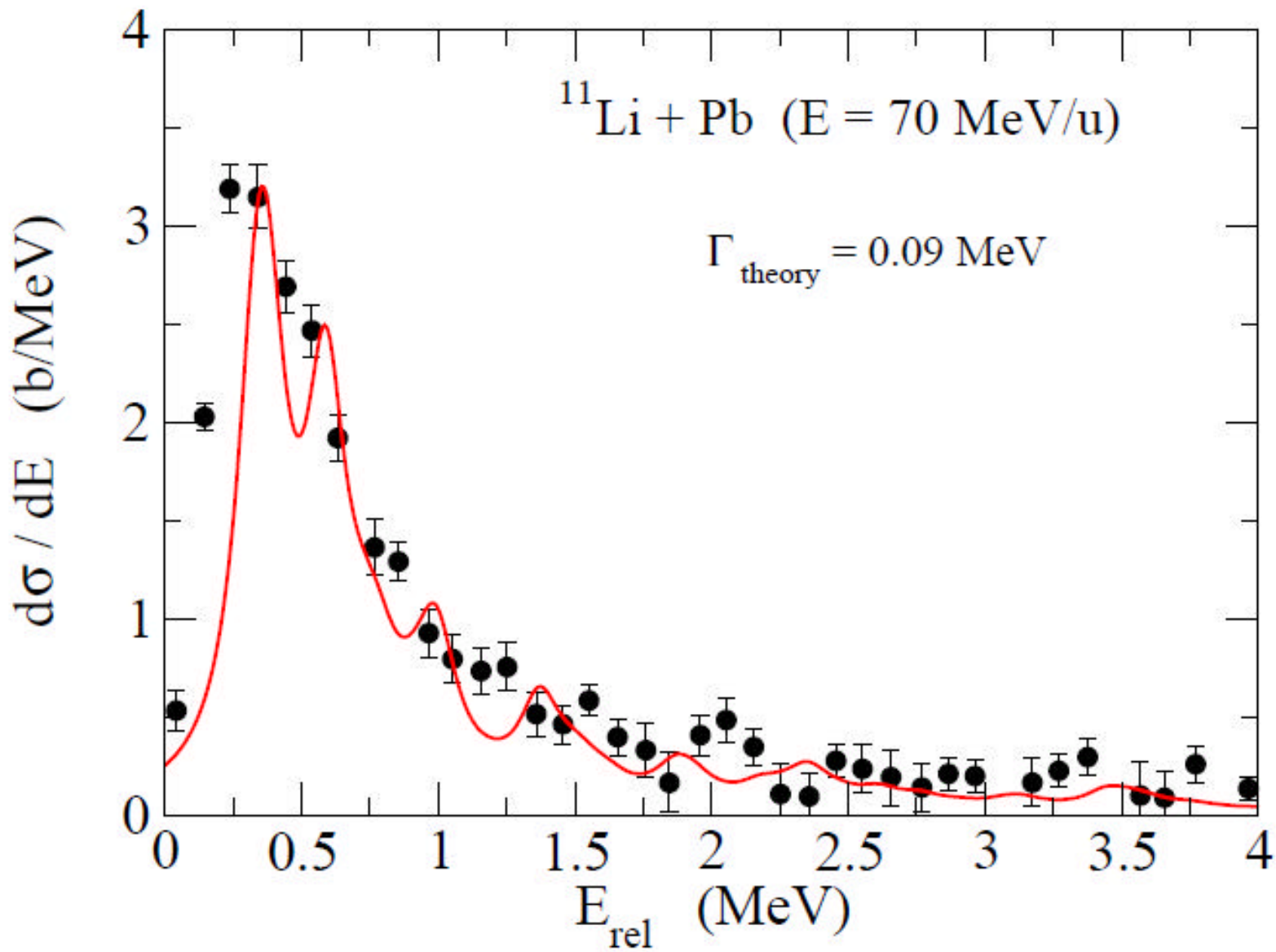
Parity Violation Electron scattering (Polarized electron beam)

Coulomb break-up reaction. (**Electric Dipole Excitations**)

Two-neutron transfer reactions.







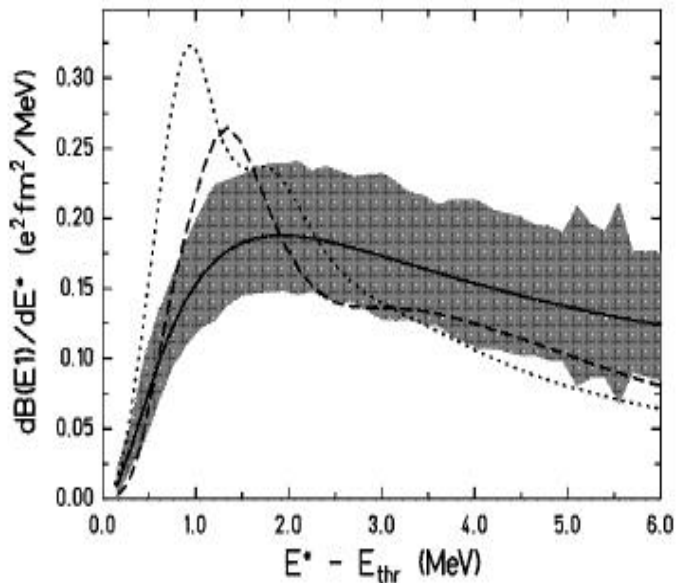
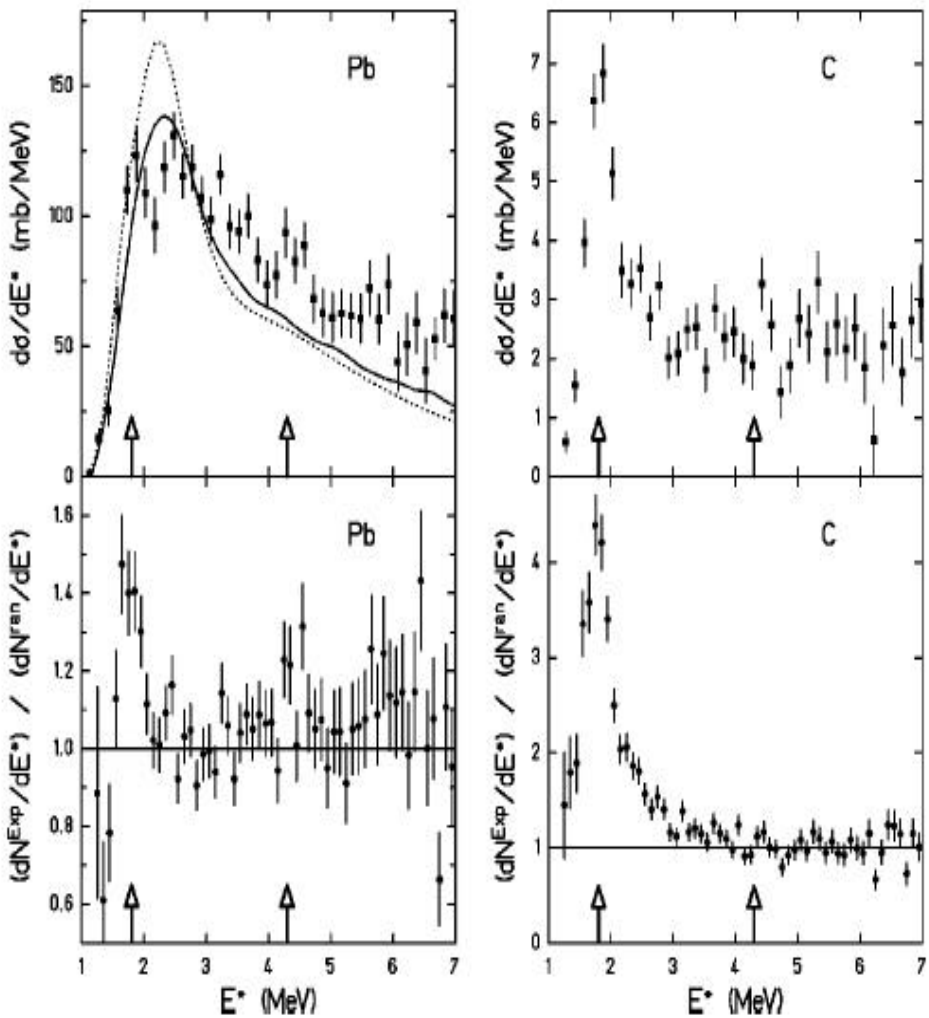
Sum rule strength in ^{11}Li

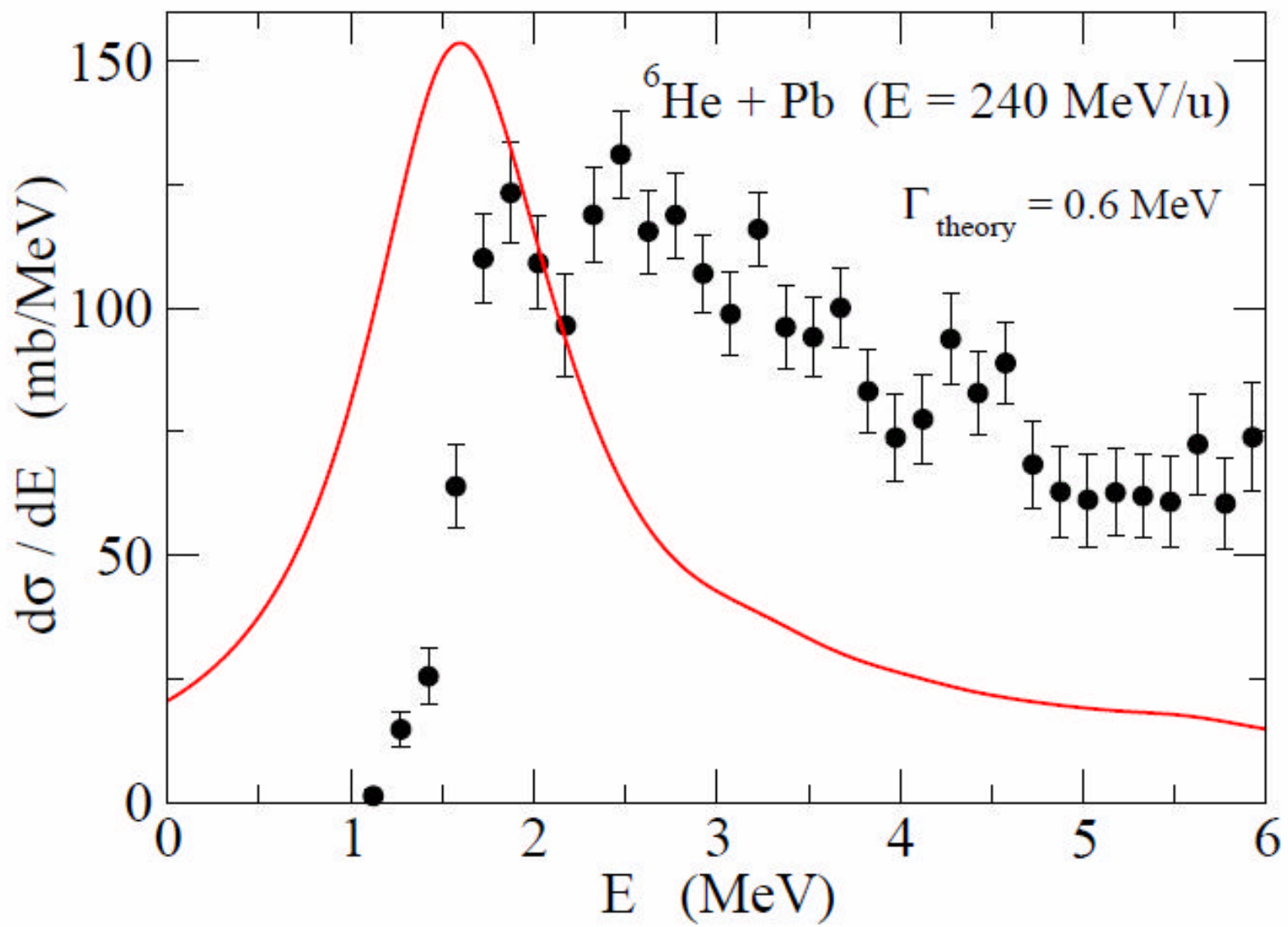
Exp: $\text{Ex} < 3.3\text{MeV}$ $B(E1) = (1.5 \pm 0.1)\text{e}^2\text{fm}^2$

Cal: $\text{Ex} < 3.3\text{MeV}$ $B(E1) = 1.31 \text{ e}^2\text{fm}^2$

Continuum Energy Spectrum of ${}^6\text{He}$ above alpha+2n threshold

T. Aumann et al., PRC59, 1259(1999)





Ref.	$\Sigma B(E1)$ (e^2 fm 2)	$\Sigma E^{**} B(E1)$ (e^2 fm 2 MeV)
Expt. ($E^* \leq 5$ MeV)	0.59 ± 0.12	1.9 ± 0.4
[7] ($E^* \leq 5$ MeV)	0.71	2.46
Expt. ($E^* \leq 10$ MeV)	1.2 ± 0.2	6.4 ± 1.3
[7] ($E^* \leq 10$ MeV)	1.02	4.97
Cluster sum rule	1.37 [7]	4.95
TRK sum rule		19.7
Present ($E < 5$ MeV)	0.71	1.49
($E < 10$ MeV)	0.95	3.22

Experimental proof of di-neutron and/or molecule-type configurations

Coulomb breakup reactions

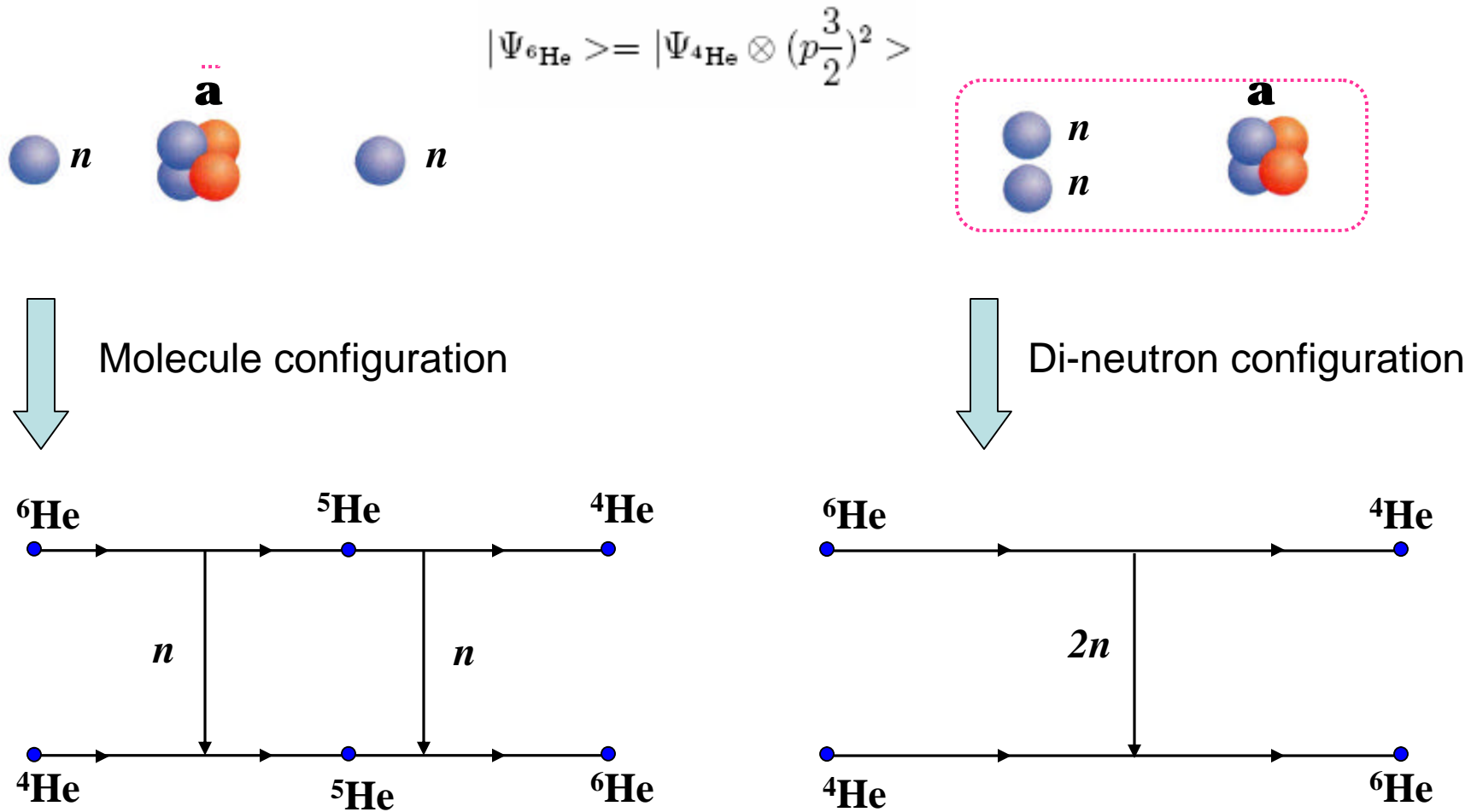
Dipole strength

2n transfer reactions

(*a*, 6He)

(*p*, *t*)

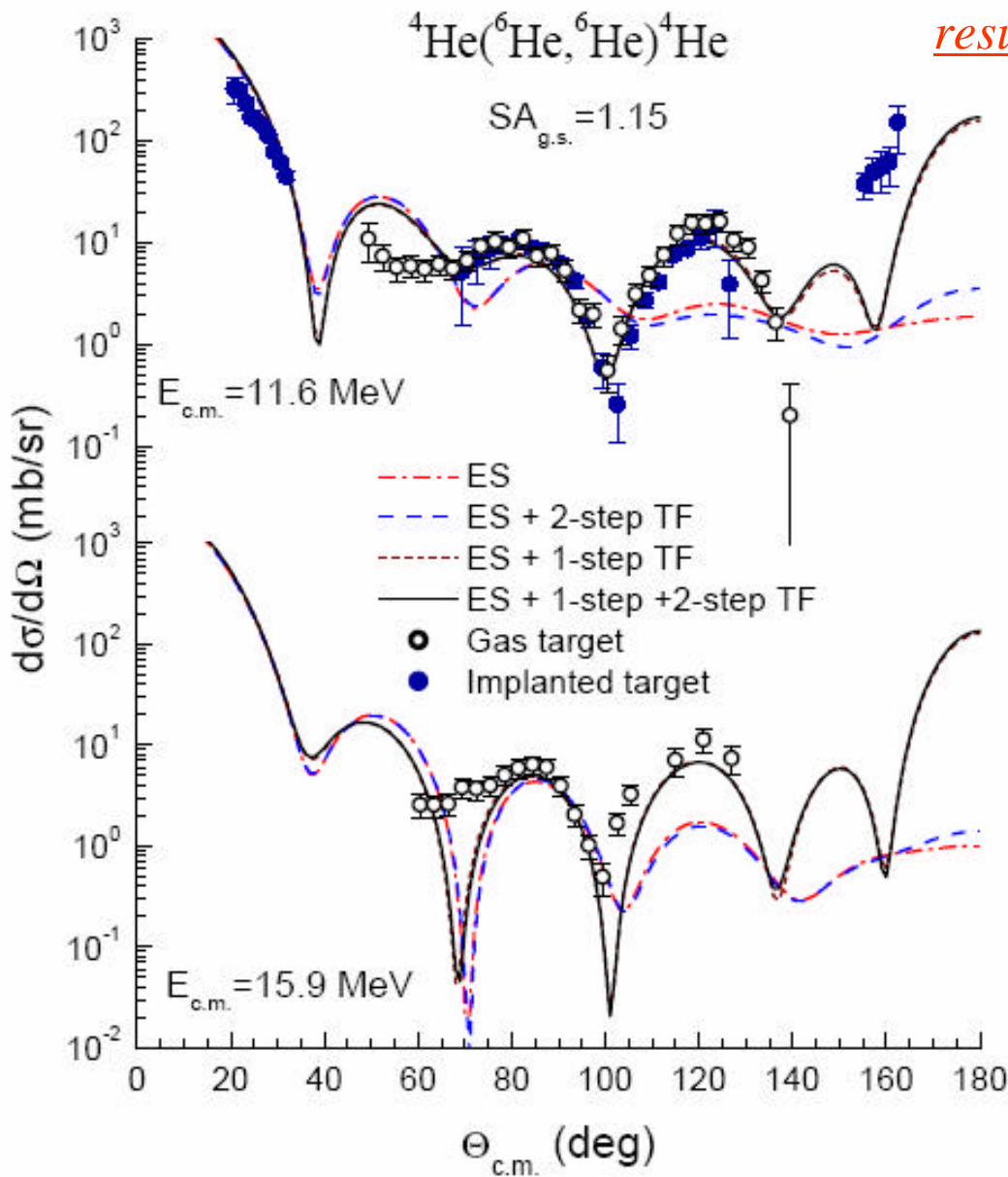
Elastic di-neutron transfer in the ${}^4\text{He}({}^6\text{He}, {}^6\text{He}){}^4\text{He}$ reaction



Sequential (two-step) transfer

Direct (one-step) transfer

Coupled Reaction Channels(CRC)
results obtained with FRESCO code



Louvain-la-Neuve data:

R. Raabe et al.,
Phys. Lett. **B458** (1999) 1;
Phys. Rev. **C67** (2003) 044602.

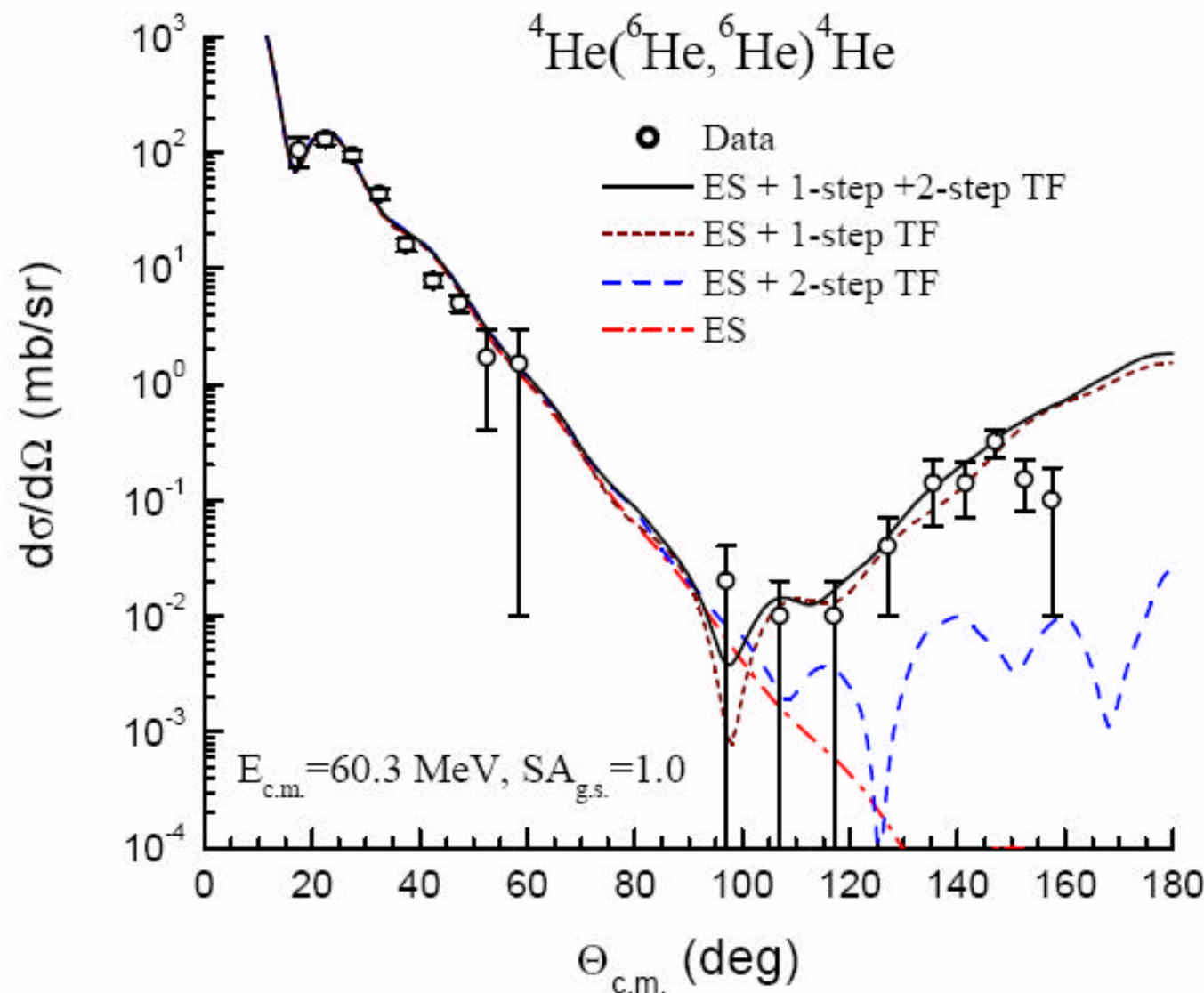
ES= Elastic scattering

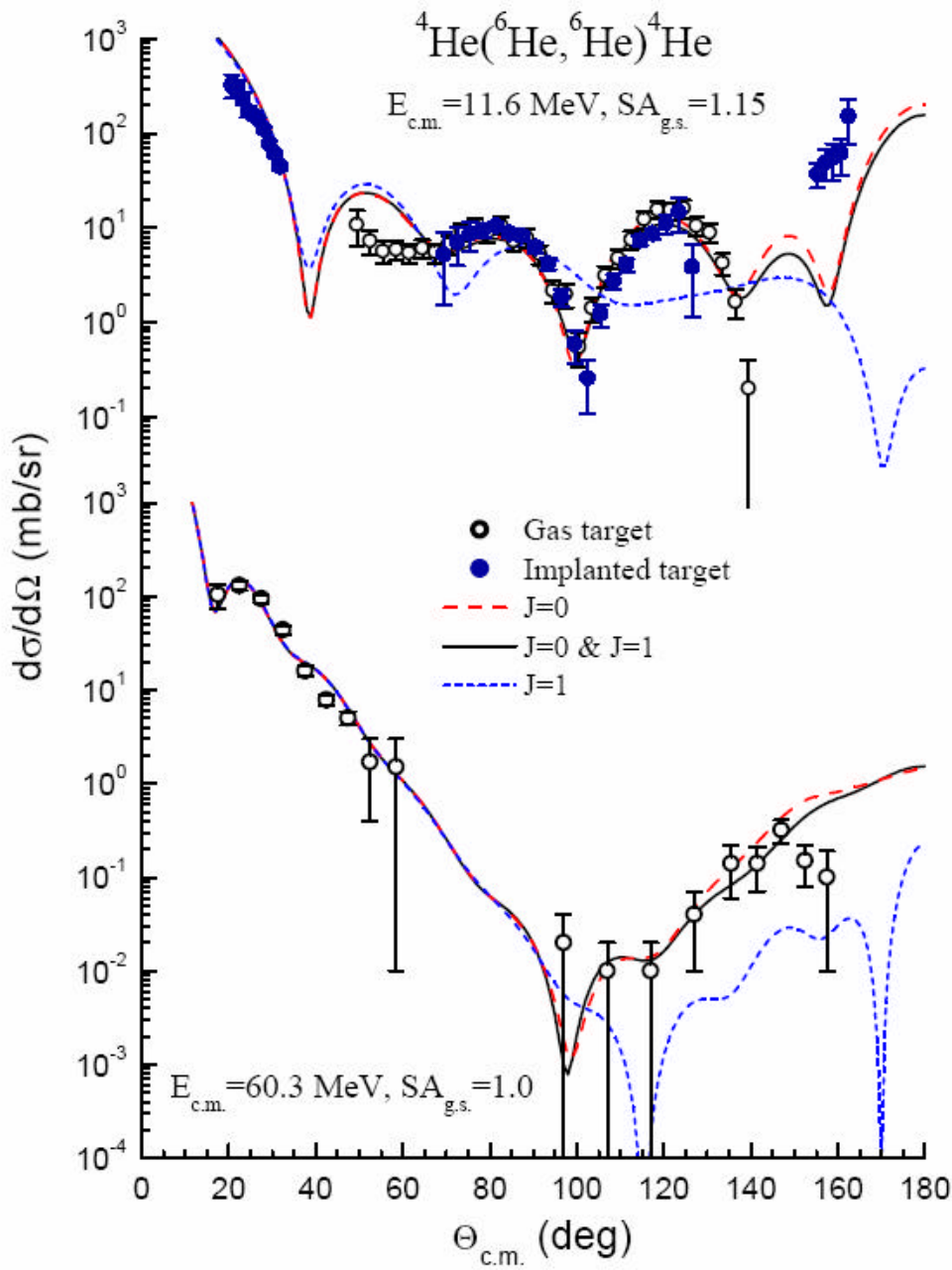
TF= $2n$ -transfer

Dominance of the
direct $2n$ -transfer !

Dubna data: G.M. Ter-Akopian et al., *Phys. Lett.* **B426** (1998) 251.

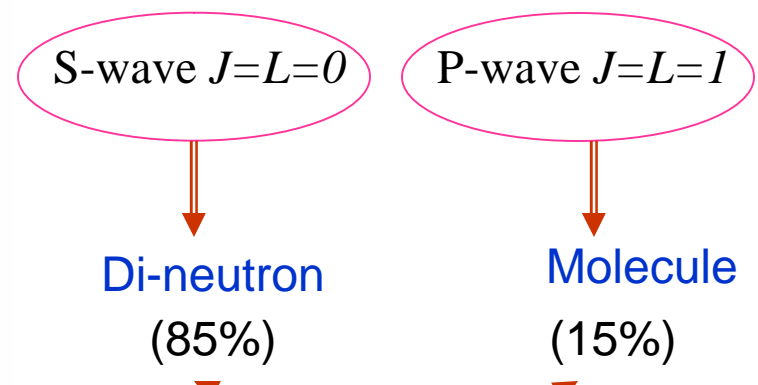
CRC analysis: D.T. Khoa and W. von Oertzen, *Phys. Lett.* **B595** (2004) 193.





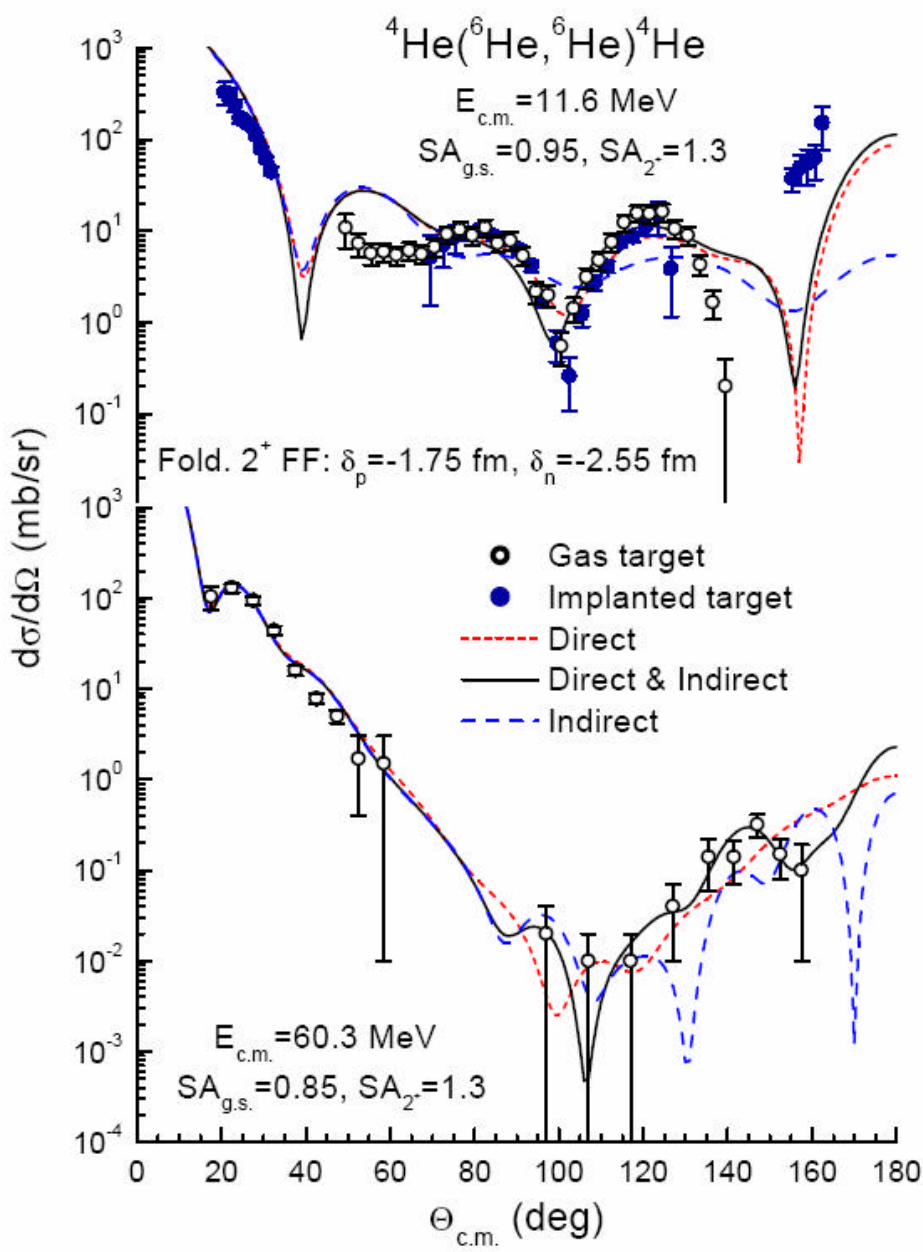
N.K. Timofeyuk,
Phys. Rev. C63 (2001) 054609

$$|\Psi_{{}^4\text{He}} \otimes (p\frac{3}{2})^2\rangle \equiv \sum |NL(nlJ); 0^+ \rangle$$

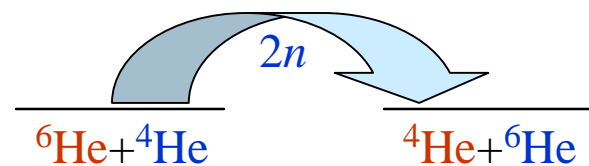


Study using the hyperspherical basis
[E. Nielsen et al., *Phys. Rep.* **347** (2001) 373]; [Cluster model](#) [D. Baye et al., *Phys. Rev. C54* (1996) 2563].

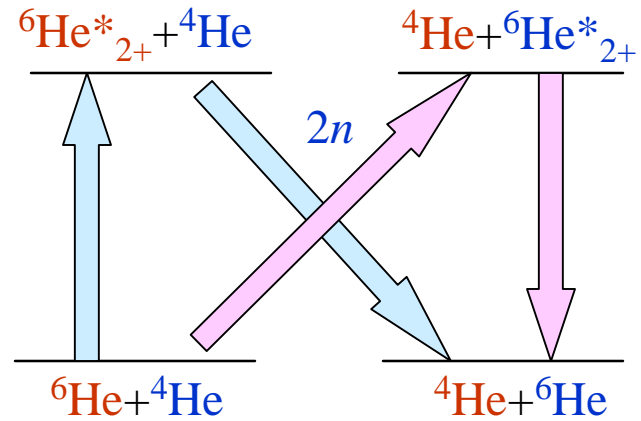
CRC results obtained with the code FRESCO (I.J. Thompson)



Direct $2n$ TF



Indirect $2n$ TF



via unbound 2^+ excitation of ${}^6\text{He}$

Summary

1. We have studied a role of di-neutron correlations in weakly bound nuclei on the neutron drip line.
2. The two peak structure is found in the borromean nuclei:
One peak with small open angle -> di-neutron
Another peak with large open angle -> H₂O molecule type correlation.
3. Di-neutron configuration is dominated by S=0, while the H₂O depends on the nuclei having either S=1 or S=0.
4. A skin nucleus ²⁴O shows no clear separation of the two configurations.
5. Dipole excitations show strong threshold effect in the borromеans, while there is no clear sign of the continuum coupling in the skin nucleus.
6. The threshold effect is dominated by the S=0 wave functions.
on the other hand, the coherent sum of S=0 and S=1 states enhances the dipole strength in ²⁴O .
7. Possible experimental probe Coulomb excitation, 2n transfer,

Future Perspectives

1. S=1 correlations: parity doublets.
2. Angular correlations of two-neutron breakup reactions.
3. Two-proton halo ^{19}F .